

# Dynamical evolution and chronology of the Hygiea asteroid family

V. Carruba<sup>1\*</sup>, R. C. Domingos<sup>2</sup>, M. E. Huaman<sup>1</sup>, C. R. dos Santos<sup>1</sup>, and D. Souami<sup>3,4,5</sup>

<sup>1</sup>UNESP, Univ. Estadual Paulista, Grupo de dinâmica Orbital e Planetologia, Guaratinguetá, SP, 12516-410, Brazil

<sup>2</sup>INPE, Instituto Nacional de Pesquisas Espaciais, São José dos Campos, SP, 12227-010, Brazil

<sup>3</sup>NAXYS, Namur Center for Complex Systems, Department of Mathematics, University of Namur, 5000 Namur, Belgium

<sup>4</sup>UPMC, Université Pierre et Marie Curie, 4 Place Jussieu, 75005, Paris, France

<sup>5</sup>SYRTE, Observatoire de Paris, Systèmes de Référence Temps Espace, CNRS/UMR 8630, UPMC, Paris, France;

Accepted 2013 October 21. Received 2013 October 18; in original form 2013 August 20

## ABSTRACT

The asteroid (10) Hygiea is the fourth largest asteroid of the Main Belt, by volume and mass, and it is the largest member of its own family. Previous works investigated the long-term effects of close encounters with (10) Hygiea of asteroids in the orbital region of the family, and analyzed the taxonomical and dynamical properties of members of this family. In this paper we apply the high-quality SDSS-MOC4 taxonomic scheme of DeMeo and Carry (2013) to members of the Hygiea family core and halo, we obtain an estimate of the minimum time and number of encounter necessary to obtain a  $3\sigma$  (or 99.7%) compatible frequency distribution function of changes in proper  $a$  caused by close encounters with (10) Hygiea, we study the behavior of asteroids near secular resonance configurations, in the presence and absence of the Yarkovsky force, and obtain a first estimate of the age of the family based on orbital diffusion by the Yarkovsky and YORP effects with two methods.

The Hygiea family is at least 2 Byr old, with an estimated age of  $T = 3200^{+380}_{-120}$  Myr and a relatively large initial ejection velocity field, according to the approach of Vokrouhlický *et al.* (2006a, b). Surprisingly, we found that the family age can be shortened by  $\simeq 25\%$  if the dynamical mobility caused by close encounters with (10) Hygiea is also accounted for, which opens interesting new research lines for the dynamical evolution of families associated with massive bodies. In our taxonomical analysis of the Hygiea asteroid family, we also identified a new V-type candidate: the asteroid (177904) (2005 SV5). If confirmed, this could be the fourth V-type object ever to be identified in the outer main belt.

**Key words:** Minor planets, asteroids: general – Minor planets, asteroids: individual: Hygiea – Celestial mechanics.

## 1 INTRODUCTION

The asteroid (10) Hygiea is the fourth largest asteroid of the Main Belt, by volume and mass, and it is the largest member of its own family. The long-term effect of close encounters of asteroids in the orbital region of the Hygiea family was recently investigated in Carruba *et al.* (2013a), that found surprisingly high values of drift rates of changes in proper semi-major axis caused by this mechanism of dynamical mobility. A preliminary taxonomical analysis and review of physical and dynamical properties of local asteroids was performed in Carruba (2013) (paper I hereafter), that found a somewhat limited role for secular dynamics in

the region of the Hygiea family, core and halo. In this work we try to answer some of the questions posed by these two earlier papers, and in particular we apply for the first time the high-quality taxonomy scheme described in the recently submitted paper of DeMeo and Carry (2013) to asteroids in the region, to eliminate all possible taxonomical interlopers. We extend the simulations carried out in Carruba *et al.* (2013a) (paper II hereafter) to get an estimate of the minimum number of close encounters needed to obtain a  $3\sigma$ -level (or 99.7%) approximation of the probability distribution function (*pdf*) of changes in proper  $a$  caused by close encounters with (10) Hygiea. We studied the actual behavior of the “likely resonators” identified in paper I to check for the fraction of objects currently in resonant states, with and without the Yarkovsky force. We obtain for the first time an

\* E-mail: vcarruba@feg.unesp.br

estimate of the age of the Hygiea family core and halo, with two independent methods, by considering the evolution of asteroids semi-major axis under the Yarkovsky and YORP effects. Then, we evaluate the effect that dynamical mobility caused by close encounters with (10) Hygiea has on the estimated age of the family.

In this work we used values of asteroid proper elements, frequencies, photometry, and albedos obtained from public databases. The synthetic proper elements and frequencies are available at the AstDyS site <http://hamilton.dm.unipi.it/cgi-bin/astdys/astibo>, accessed on May 15<sup>th</sup>, 2013 (Knežević and Milani 2003) We used photometric data from the Sloan Digital Sky Survey-Moving Object Catalog data, fourth release (SDSS-MOC4 hereafter, Ivezić et al. 2002), that provided multi-band photometry for a sample two order of magnitude larger than any current available in spectroscopic catalogs (about 60000 numbered objects). Finally, results from the Wide-field Infrared Survey Explorer (WISE) (Wright et al. 2010), and the NEOWISE (Mainzer et al. 2011) enhancement to the WISE mission recently allowed to obtain diameters and geometric albedo values for more than 100,000 Main Belt asteroids (Masiero et al. 2011), increasing the sample of objects for which albedo values are known by a factor 50.

This work is so divided: in Sect. 2 we identified members of the Hygiea family core and halo using the new taxonomical scheme of DeMeo and Carry (2013). In Sect. 3 we studied the long-term effect of close encounters of asteroids in the orbital region of (10) Hygiea with (10) Hygiea itself. Sect. 4 is dedicated to the analysis of the dynamical evolution caused by secular dynamics in the Hygiea family orbital region. In Sect. 5 we estimated the age of the Hygiea family when evolution in semi-major axis caused by Yarkovsky and YORP effects is considered. In Sect. 5.3 we considered how close encounters affected the estimate of the family age. Finally, in Sect. 6 we present our conclusions.

## 2 HYGIEA FAMILY: IDENTIFICATION AND TAXONOMY

The Hygiea family was most recently identified in the domain of proper elements ( $a, e, \sin(i)$ ), in several domains of proper frequencies (Carruba 2013), and in a multi-domain of proper elements, SDSS-MOC4 ( $a^*, i-z$ ) colors, and WISE geometrical albedo by Carruba et al. (2013b). DeMeo and Carry (2013) recently introduced a new classification method, based on the Bus-DeMeo taxonomic system, that employs SDSS-MOC4 gri slope and  $z' - i'$  colors. In that article the authors used the photometric data obtained in the five filters  $u', g', r', i'$ , and  $z'$ , from 0.3 to 1.0  $\mu m$ , to obtain values of  $z' - i'$  colors and spectral slopes over the  $g', r'$ , and  $i'$  reflectance values, computed using the equation:

$$R_f = 10^{-0.4[(M_f - M_g) - (M_{f, sun} - M_{g, sun})]}, \quad (1)$$

where  $M_f$  and  $M_{f, sun}$  are the magnitudes of the object and the sun in a certain filter  $f$ , respectively, at the central wavelength of that filter. The equation is normalized to unity at the central wavelength of filter  $g$  using ( $M_g$ ) and  $M_{g, sun}$ , the  $g$  magnitudes of the object and the sun, respectively. Values of the solar colors  $r' - g' = -0.45 \pm 0.02$ ,  $i' - g' = -0.55 \pm 0.03$ ,

and  $z' - g' = -0.61 \pm 0.04$  are taken from Holmberg et al. (2006).

DeMeo and Carry (2013) defined strict criteria to reject flawed observation: they eliminated from the SDSS-MOC4 database objects with a provisional designation, observations with unreliable magnitudes in any of the five filters, values of the  $u'$  filter (also because of the large errors associated with measurements in this wavelength band), and data with flags relevant to moving objects and good photometry. We refer the reader to Sect. 2 of DeMeo and Carry (2013) for more details on the criteria used to obtain high quality measurements from SDSS-MOC4 data.

We applied the methods described in DeMeo and Carry (2013) to the SDSS-MOC4 dataset. We refer the reader to Fig. 5 in DeMeo and Carry (2013), that displays the boundaries, in the plane  $gri$  slope (measured in the standard units of  $\%/100 nm$ ) versus  $z' - i'$  colors, used to classify SDSS-MOC4 data into the taxonomic classes of the Bus-DeMeo taxonomy, converted to SDSS-MOC4 gri slopes and  $z' - i'$  colors. We also assigned numbers to the objects that, at the time of the release of SDSS-MOC4 had only temporary designation and received numbers since then (a total of 7234 asteroids), and, as in DeMeo and Carry (2013), we eliminated all objects with  $H > 15.30$ , so as to avoid including objects with  $D < 5$  km, for which the sample is incomplete. Also, we included asteroids with  $H < 12.00$  with known spectral types from the Planetary Data System (Neese 2010) that are not part of SDSS-MOC4.

As a first part of our analysis, we checked if the preliminary analysis of the taxonomy of the Hygiea family halo performed in paper I still holds. In that article it was found that the composition of the Hygiea family as deduced from principal components obtained from SDSS-MOC4 photometry was very similar to that of the nearby Themis and Veritas families, all belonging to CX-complex taxonomies. Therefore, it was somewhat difficult to determine, based only on taxonomical considerations, if a member of the Hygiea family halo (or indeed of the family core itself) was a fragment of the Hygiea parent body or a member of the two other families that dynamically migrated to its present orbital location. Here we applied the more advanced taxonomical scheme of DeMeo and Carry (2013) to members of the cores of the Hygiea, Themis, and Veritas families computed at a conservative cutoff value of 50 m/s (or distance) in the proper element domain, and that also have data in the reduced SDSS-MOC4 sample. Fig. 1 displays proper ( $a, \sin(i)$ ) projection (panel A) and a  $gri$  slope versus  $z' - i'$  plane projection, superimposed to the boundaries of the DeMeo and Carry classification (panel B), of members of the core of the Veritas (red asterisks), Hygiea (black dots), and Themis (blue circles) asteroid families.

We believe that our results essentially confirm the preliminary analysis of paper I: most of the members of the Hygiea, Themis and Veritas families belong to the C- and X- type, with a fraction of Hygiea and Themis family members that can be classified as B-types. Essentially, C- and X- type members of the Hygiea family halo that may have come from the Themis or Veritas families are indistinguishable from halo member that came from the parent body of (10) Hygiea itself. B-type asteroids in that halo may either come from the Hygiea or Themis families, but not from the Veritas one. Eliminating possible Themis or Veritas families

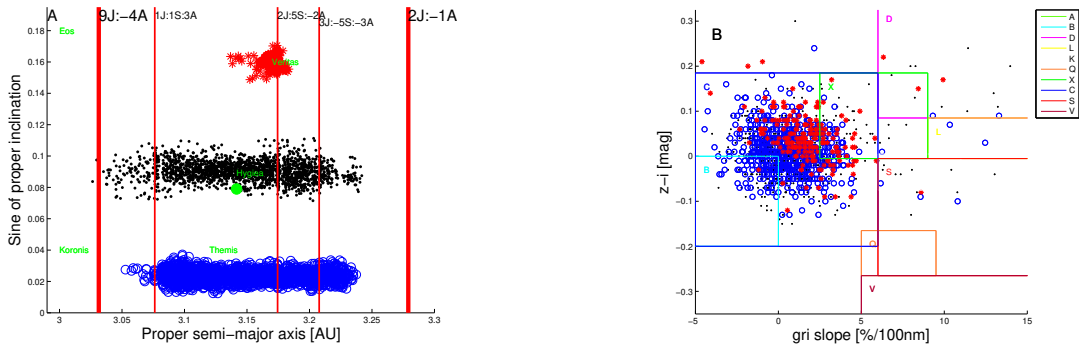


**Figure 1.** A proper ( $a, \sin(i)$ ) projection of members of the core of the Veritas (red asterisks), Hygiea (black dots), and Themis (blue circles) asteroid families, computed at a cutoff of 50 m/s in the proper element domain (panel A). A projection of the same asteroids in the  $gri$  slope versus  $z' - i'$  plane, superimposed to the boundaries of the DeMeo and Carry classification (panel B).

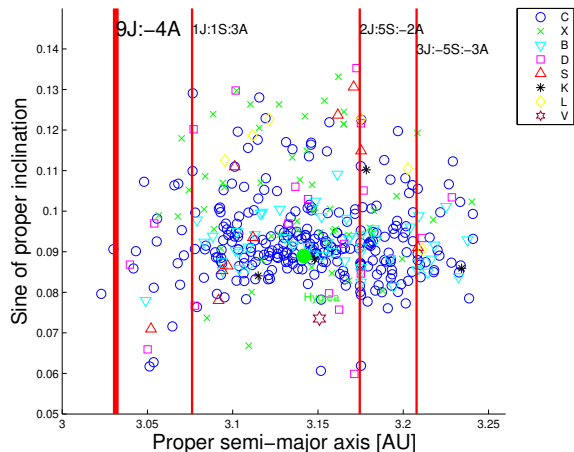


**Figure 2.** A proper ( $a, \sin(i)$ ) projection of asteroids in the Hygiea family halo with an identifiable SDSS-MOC4 taxonomy, according to the DeMeo and Carry (2013) scheme.

interlopers in the Hygiea family halo based on taxonomical considerations only seems, therefore, somewhat unlikely.

Since our focus in this paper is to study the Hygiea asteroid family, we selected objects in the SDSS-MOC4 reduced dataset that were members of the Hygiea family core and halo, as obtained at velocities cutoffs of 66 and 76 m/s in paper I. We found a total of 497 observations in the Hygiea family core and 695 observations in the Hygiea family halo. A taxonomy is given according to the method described in DeMeo and Carry (2013), i.e., if the  $z' - i'$  and  $gri$  slope is found in the region boundary of a class then the asteroid is assigned to that class. For overlapping classes, the taxonomy is assigned in the last class in which the object resides, in the following order: C-, B-, S-, L-, X-, D-, K-, Q-, V-, and A-types. Since some asteroids had multiple observations in the SDSS-MOC4 database, we adopted the DeMeo and Carry (2013) criteria for classifications in this cases: in case of conflicts, the class with the majority number of classifications is assigned. If two classes have equal frequency, preference is given to C-, S-, or X-type classifications. If the two majority classes are C/S, X/C or S/X, or there is no majority, no class is assigned to this object (class U in the DeMeo and Carry (2013) paper).

Table 1 displays the number of C-, X-, B-, D-, K-, S-, L-, and U- type objects in the hygiea family core and halo, whose orbital projection in the plane of proper ( $a, \sin(i)$ ) is given in Fig. 2. We also, very surprisingly, identified one possible V-type object, the asteroid 177904 (2005 SV5), that, to our knowledge, could be the fourth V-type object found in the outer main belt after the well known case of (1459) Magnya, and (7472) Kumakiri and (10537) (1991 RY16) (Duffard 2009). According to the mineralogic analysis of Mothé-Diniz et al. (2005), D-, S-, K-, V-, A- and U- type objects are to be considered interlopers for taxonomical reasons and will not be considered part of the family, made mostly by B-, C-, and X-type objects, for what concerns its age determination. This analysis left us with 276 and 376  $D > 5$  km asteroids in the Hygiea family core and halo, respectively. The mean WISE albedo of the Hygiea family core members was of 0.0576, with a minimum value of 0.0245 and a maximum of 0.189<sup>1</sup>. These results are compatible with what observed for typical C- and B- type classes in DeMeo and Carry (2013).

Having obtained a determination of the orbital boundaries of the Hygiea family, we are now ready to start studying orbital dispersion mechanisms such as the long-term effect of close encounters with (10) Hygiea. This will be the subject of the next section.

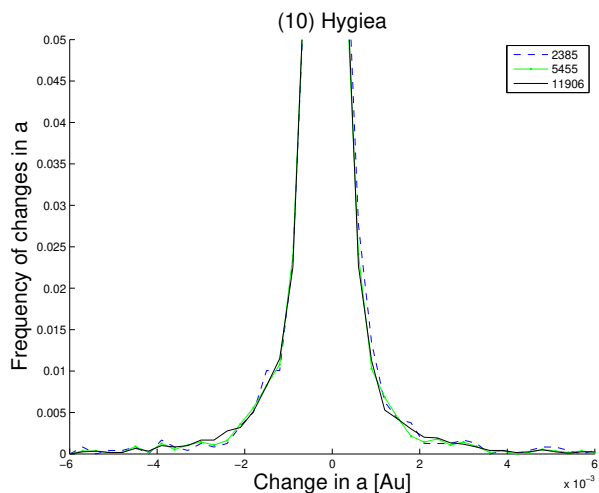
### 3 LONG-TERM EFFECT OF CLOSE ENCOUNTERS WITH (10) HYGIEA: PROBABILITY DISTRIBUTION FUNCTION

The long-term effect of close encounters of asteroids in the orbital region of (10) Hygiea with (10) Hygiea itself was most recently studied by paper II. In that article, the authors found that the frequency distribution functions ( $fdf$ ) of changes in proper  $a$  caused by close encounters tested positive against the null hypothesis at a  $2\sigma$ -level, or 95.4% probability level, for number of encounters larger than 4500,

<sup>1</sup> Since WISE albedo values tend to be higher than usually expected for small objects, we eliminated from our sample four asteroids with geometric albedos higher than 0.2, a value this not usually associated with C-, X-, and B- type asteroids. Including these asteroids in our sample yields the slightly higher value of mean WISE albedo of 0.078.

**Table 1.** Number of C-, X-, B-, D-, K-, S-, L- and U- type objects in the Hygiea family core and halo.

Group	# of C-types	# of X-types	# of B-types	# of D-types	# of K-types	# of S-types	# of L-types	# of U-types
Hygiea core	206	28	42	7	4	4	0	10
Hygiea halo	270	56	50	19	4	10	6	16

**Figure 3.** Histogram of frequency of changes in proper  $a$  caused by close encounters with (10) Hygiea.

and were expected to be compatible amongst them at a  $3\sigma$ -level, or 99.7% probability level, for number of encounters larger than  $\simeq 6000$ , based on analytical considerations obtained using Greenberg (1982) model of the effect of changes in heliocentric velocities caused by close encounters. Essentially, the higher the number of encounters, the better the phase space of minimum distance and relative velocity at encounter, the two parameters that dictate the change in heliocentric velocity of the asteroid, and, therefore, of proper elements, the more precise the approximation of the  $fdf$  to the real probability distribution function (or  $pdf$ ). The actual minimum number of encounters needed to obtain a  $3\sigma$ -level approximation of the  $pdf$  was, however, not tested in that work.

To verify the actual number of close encounters needed to obtain a  $3\sigma$ -level approximation of the  $pdf$ , we performed a simulation with 7015 particles belonging to the Hygiea family halo as identified in paper I. Since paper II showed that, for the purpose of obtaining a good estimate of the  $pdf$  results obtained also including the Yarkovsky effect are not quantitatively different from those obtained with simulations without such effect, we limited our modeling to the effect of close encounters with (10) Hygiea. The 7015 particles were integrated under the influence of the eighth planets and the four most massive bodies in the main belt, (1) Ceres, (2) Pallas, (4) Vesta, and (10) Hygiea, over 34 Myr using the SWIFT-SKEEL code of the SyMBA package of Levison and

Duncan (1994), modified to monitor each encounter that occurred between (10) Hygiea and the test particle at a distance of less than  $1 \cdot 10^{-3}$  AU and with a time step of 2 days (see Carruba et al. (2012) for a discussion on the reasons for choosing these two parameters). Since the standard deviation of changes obtained in the absence of encounters with (10) Hygiea is of the order of  $2 \cdot 10^{-4}$  AU, we concentrated our attention on encounters that caused a change in  $a$  at least three times this value, since these are more significant for the dynamical mobility caused by close encounters with massive asteroids (Carruba et al. 2003), and are less likely to be caused by other effects.

Fig. 3 displays a histogram of frequency of changes in proper  $a$  caused by close encounters with (10) Hygiea for our simulated particles. As in paper II we performed Kolmogorod-Smirnoff probability tests (KS tests hereafter) for each of the observed distributions at confidence levels of  $2\sigma$  and  $3\sigma$  between the whole distribution of 11906 encounters occurred during the simulation, and sub-samples of encounters, in the regions of changes in  $a$  of most interest, i.e.,  $0.0006 < |\Delta a| < 0.006$  AU. We found that sub-samples of encounters start to be compatible at  $2\sigma$  level for 2385 encounters, and at a  $3\sigma$  level for 5455 number of encounters, that is in remarkable good agreement with what predicted in paper II. The frequency distribution functions of  $\Delta a$  for the 2385 and 5455 encounters are also displayed in Fig. 3.

In Sect. 2 we identified 276 and 376 taxonomically compatible asteroids in the Hygiea family core and halo, respectively. How much time would be necessary for these populations of asteroids to experience number of encounters such that the  $fdf$  in  $\Delta a$  could converge to the  $pdf$ , at least at a  $2\sigma$  confidence level? To answer this question, we computed the number of encounter experienced by these two populations during the 34 Myr integration, as a function of time, and extrapolated these values with simple linear laws.

Fig. 4 displays the number (line) and expected number (dotted line) of encounters with (10) Hygiea for the population of objects with  $H < 15.3$  in the Hygiea family core (blue lines) and halo (red lines). To reach a number of 2385 encounters, sufficient to attain a  $2\sigma$  level in the approximation of the  $pdf$ , it is expected that it will take 113.1 Myr for the halo population and 162.3 Myr for the core. We will further investigate the importance of these time-scales in Sect. 5. In the next section we will bring our attention to the importance of secular dynamics in the Hygiea region.

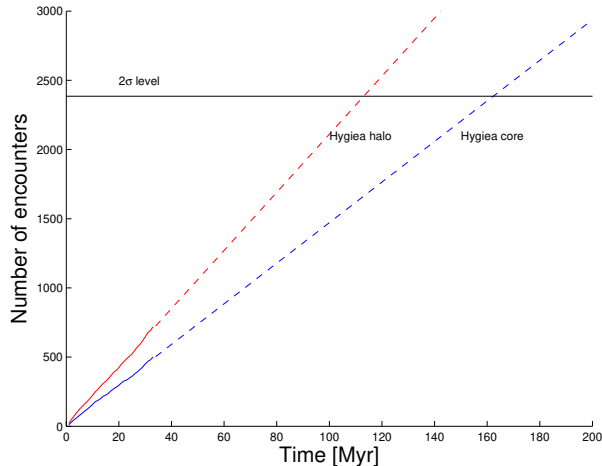


**Figure 4.** Number (line) and expected number (dotted line) of encounters with (10) Hygiea for the population of objects with  $H < 15.3$  in the Hygiea family core (blue lines) and halo (red lines).

#### 4 SECULAR DYNAMICS IN THE HYGIEA REGION

A preliminary analysis of secular dynamics in the region of the Hygiea family was already performed in paper I. In that work the author identified the population of likely resonators, i.e., the asteroids within  $\pm 0.3 \text{ arcsec/yr}$  from the resonance center (for example, in the case of the  $z_1$  secular resonance, a  $g + s$  kind of resonance in the notation of Machuca and Carruba (2011), likely resonators would be objects whose combination of  $g + s$  would fall to within  $\Delta_{gs} = 0.3 \text{ arcsec/yr}$  from the resonance center, i.e.  $g + s = g_6 + s_6 \pm \Delta_{gs}$ ). Limitations of that approach are however that i) the  $0.3 \text{ arcsec/yr}$  limit was derived for the  $z_1$  resonance, and may differ for other secular resonances, ii) the fact that an asteroid is a likely resonator does not guarantee that it is in a librating state, and iii) the method used to obtain synthetic proper elements may produce values of proper frequencies close to resonant values, even for asteroids in circulating states. In order to obtain a better understanding of secular dynamics in the region, we integrated all the population of likely resonators identified in paper I over 10 Myr with a Burlisch-Stoer integrator from the SWIFT package (Levison and Duncan, 1994) modified by Brož (1999) so as to include on-line digital filtering to remove all frequencies with period less than 600 yr, under the influence of the eight planets. We then obtained the resonant argument of each resonance discussed in paper I, and verified which asteroids were actually in librating states. Results are summarized in Table 2. With respect to what found in paper I we notice that the population of actual resonators in secular resonances that cross the Hygiea family is indeed quite limited, with the largest population of just six objects in states that alternate between libration and circulation of the  $\nu_5 + 2\nu_{16}$  secular resonance. No asteroids in pure librating states were identified for this resonance. The population of librators is actually present in larger numbers for resonances that cross the Eos family orbital region, such as the  $3\nu_6 - 2\nu_5$  (16 objects), the  $2\nu_5 - 2\nu_6 + \nu_{16}$  (69 librators), and the  $\nu_6 + \nu_{16}$  (66 objects) secular resonances.

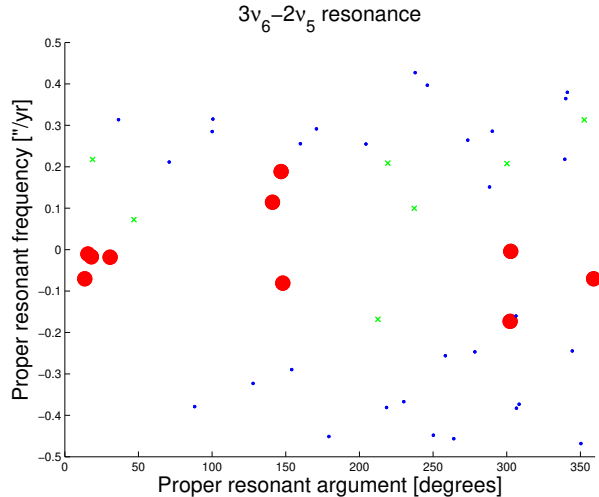


**Figure 5.** A projection in the plane  $(\varpi + 2 \cdot \varpi_5 - 3 \cdot \varpi_6, g + 2g_5 - 3g_6)$  of asteroids in librating states (red full dots), circulating states (blue dots), and alternating phases of librations and circulations (green asterisks).

To investigate the width of each of the major secular resonances observed in the region (for our purposes those with more than five observed librators) we used a resonant representative plane defined, as in Vokrouhlický et al. (2006b) and in Carruba (2009a) by the critical angle  $\sigma$  of each resonance and its conjugated frequency  $d\sigma/dt (= g + s - g_6 + s_6)$  for the  $\nu_6 + \nu_{16}$  resonance), computed considering the effect of gravitational forces only. We proceed as follows to compute these quantities: i) the orbital elements, results of the numerical simulation, are used to obtain equinoctial, non-singular elements of the form  $(e \cdot \cos \varpi, e \cdot \sin \varpi)$ , and  $(\sin(i/2) \cos \Omega, \sin(i/2) \sin \Omega)$ ; ii) the equinoctial elements of the test particles and of Jupiter, Saturn, and Uranus, are then Fourier filtered to obtain the  $g, s, g_5, g_6, s_6$  frequencies and their associated phases (see also Carruba 2010b for details on the method); iii) the frequencies are then plotted on the ordinates and their phases are used to construct the resonant angle  $\sigma$ .

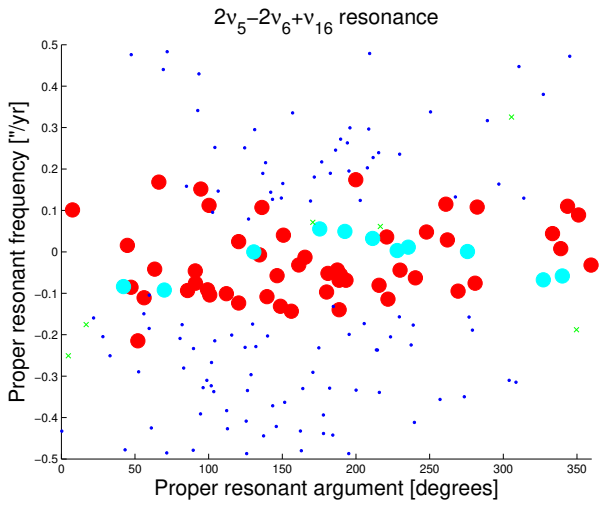
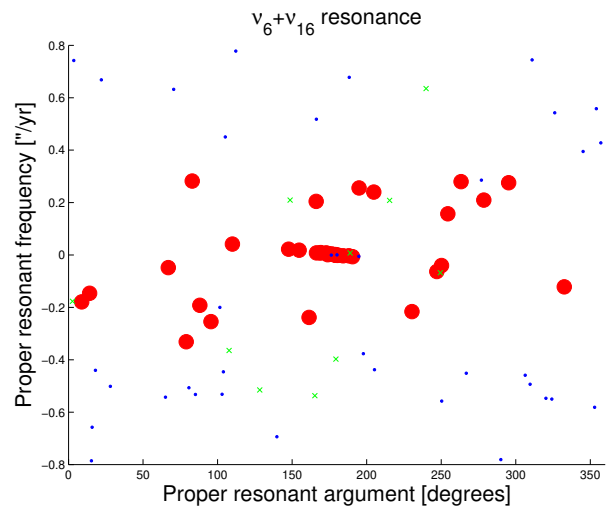
Fig. 5 displays our results for the  $3\nu_6 - 2\nu_5$  secular resonance, where asteroids in librating states are shown as red full dots, those in circulating states are marked as blue dots, and the asteroids alternating phases of librations and circulations are displayed as green asterisks. We found that the width of the region populated by librating asteroids is defined by  $g = (3g_6 - 2g_5)_{-0.173''/yr}^{+0.188''/yr}$ , i.e., less than the  $0.3 \text{ arcsec/yr}$  criteria used for the  $z_1$  resonance.

Fig. 6 displays the resonance representative plane for the  $2\nu_5 - 2\nu_6 + \nu_{16}$  secular resonance, where we also identified a new class of librating objects, oscillating around  $270^\circ$ . The width of the region populated by librating asteroids is defined by  $g = (s_6 + 2g_5 - 2g_6)_{-0.215''/yr}^{+0.174''/yr}$ , once again, less than the  $0.3 \text{ arcsec/yr}$  criteria used for the  $z_1$  resonance.

Fig. 7 displays the resonance representative plane for the  $\nu_6 + \nu_{16}$  secular resonance. Compatibly with what was found in Carruba (2009a), the width of the region populated by librating asteroids is defined by  $g = (g_6 + s_6)_{-0.282''/yr}^{+0.331''/yr}$ , i.e., in agreement with the  $0.3 \text{ arcsec/yr}$  criteria used in paper I.

**Table 2.** Main secular resonances in the Hygiea region, frequency value, number of resonant asteroids, and limit on the resonance width

Resonance argument	Frequency value <i>arcsec/yr</i>	Number of resonant asteroids	Resonance width <i>arcsec/yr</i>
g resonances			
$2\nu_6 - 2\nu_5 + \nu_7$	51.065	4	
$3\nu_6 - 2\nu_5$	76.215	16	< 0.188
s resonances			
$2\nu_5 - 2\nu_6 + \nu_{16}$	-74.317	69	< 0.215
g+s resonances			
$2\nu_5 - \nu_6 + \nu_{16}$	-46.074	1	
$\nu_5 + \nu_{16}$	-22.088	2	
$\nu_6 + \nu_{16}$	1.898	66	< 0.331
$2\nu_6 - \nu_5 + \nu_{16}$	25.884	5	
$2\nu_6 - \nu_5 + \nu_{17}$	49.233	3	
g+2s resonances			
$\nu_5 + 2\nu_{16}$	-48.433	6	< 0.127
$\nu_6 + 2\nu_{16}$	-24.447	4	
2g+s resonances			
$\nu_5 + \nu_6 + \nu_{16}$	6.155	1	

**Figure 6.** A projection in the plane  $(\Omega - \Omega_6 + 2 \cdot \varpi_6 - 2 \cdot \varpi_5, s - s_6 + 2g_6 - 2g_5)$  of asteroids in librating states (red full dots), librating states around  $270^\circ$  (cyan full dots), circulating states (blue dots), and alternating phases of libration and circulations (green asterisks).**Figure 7.** A projection in the plane  $(\varpi - \varpi_6 + \Omega - \Omega_6, g - g_6 + s - s_6)$  of asteroids in librating states (red full dots), circulating states (blue dots), and alternating phases of libration and circulations (green asterisks).

A similar analysis performed for the  $\nu_5 + 2\nu_{16}$  showed that i) there are no asteroids in pure librating states, and ii) the asteroids that had phases of libration during the simula-

tion length and that were the closest to the resonance center had a difference in resonant frequency of  $1.27 \text{ arcsec/yr}$ , which sets an upper limit on the resonance width. In the

next sub-section we will investigate what fraction of the resonant population, that we identified, remains in the resonances when non-gravitational forces such as the Yarkovsky effect are considered.

#### 4.1 Yarkovsky evolution

To investigate how effective the analyzed secular resonances are as a mechanism of dynamical mobility, we integrated the real asteroids that satisfied the preliminary frequency criterion in paper I with SWIFT-RMVSY, the symplectic integrator of Brož (1999) that simulates the diurnal and seasonal versions of the Yarkovsky effect, over 30 Myr and the gravitational influence of all planets from Venus to Neptune (Mercury was accounted for as a barycentric correction in the initial conditions). Since asteroids in the region are mostly C-type, we used values of the Yarkovsky parameters appropriate for such bodies (Carruba et al. 2003): a thermal conductivity  $K = 0.001 W/m/K$ , a thermal capacity  $C = 680 J/kg/K$ , surface density  $1500 kg/m^3$ , a Bond albedo of 0.1, a thermal emissivity of 0.95, and a bulk density of  $1500 kg/m^3$ . We used two sets of spin axis orientations with  $\pm 90^\circ$  with respect to the orbital plane, since our goal is to investigate the maximum possible diffusion of asteroids and these obliquities maximize the speed of the Yarkovsky effect. We assumed periods obtained under the approximation that the rotation frequency is inversely proportional to the object's radius, and that a 1 km asteroid had a rotation period of 5 hours (Farinella et al. 1998)<sup>2</sup>. No re-orientations were considered, so that the drift caused by the Yarkovsky effect was the maximum possible. We also used the WISE radii for the 295 asteroids for which this information was available, for the other objects we computed the radius using the equation:

$$R(km) = 664.5 \frac{10^{(-H/5)}}{\sqrt{p_V}}, \quad (2)$$

where  $H$  is the asteroid's absolute magnitude provided by the AstDyS site, and  $p_V$  is the geometric albedo, assumed equal to that of (10) Hygiea, as measured from the WISE mission ( $p_V = 0.0579$ ). We computed proper elements with the approach described in the previous section over 23 intervals of 1.2288 Myr (i.e. 2048 intervals of 600 yr, where 600 is the time interval in the output of our simulation, and  $2048 = 2^{11}$  is a power of 2 in order to perform a Fourier analysis), and checked what objects remained inside the investigated secular resonances, for how long, and what was the change in proper  $a, e, \sin(i)$  caused by the passage through

<sup>2</sup> Other choices of rotation periods are possible. One can choose a distribution of rotation frequencies similar to that of other families, and randomly choose values for each asteroid. However, Cotto-Figueroa et al. (2013) have shown that the YORP effect is extremely sensitive to the topography of the asteroid, and its small changes. We therefore believe that in the end it may make little difference what initial rotation period is chosen. The rotation period of an asteroid will change during a YORP cycle in ways that are not currently well understood. Since our goal in this section is to preliminarily investigate the fraction of surviving resonators when non-gravitational forces are considered, we believe that our simpler approach was justified.

resonance. We focused on resonances that the analysis of paper I showed more likely to affect the evolution of the Hygiea asteroid family, such as the  $\nu_5 + 2\nu_{16}$ ,  $\nu_6 + 2\nu_{16}$ ,  $2\nu_6 - \nu_5 + \nu_{16}$ , and  $2\nu_6 - \nu_5 + \nu_{17}$ . The  $3\nu_6 - 2\nu_5$ ,  $2\nu_5 - 2\nu_6 + \nu_{16}$ , and  $\nu_6 + \nu_{16}$  secular resonances were also studied because the analysis of Sect. 4 showed us that they have the largest population of actual librators in the region, despite the fact that they only marginally affect the evolution of Hygiea family asteroids.

Table 3, which reports the number of librators, mean and maximal value of time of permanence in resonance, changes in proper  $e$  and  $\sin(i)$ , for the studied resonances, summarizes our results. Secular resonances in the Hygiea family area have a limited effect on asteroid dynamics: the largest population of resonators was found inside the  $2\nu_6 - \nu_5 + \nu_{16}$  resonance, with 29 asteroids. Resonances in the Eos family area seem to have more impact on the local dynamics, which is especially true for the powerful  $\nu_6 + \nu_{16}$  secular resonance, whose effect on the Eos family was studied in Vokrouhlický et al. (2006d) and Carruba and Michtchenko (2007), among others. While the population of resonators is limited in secular resonances in the Hygiea family region, the effect of such resonances is not negligible. Maximum changes in proper eccentricity and inclination occur for particles whose orbits cross the separatrix between circulation and libration<sup>3</sup>. The relatively weak  $\nu_6 + 2\nu_{16}$  secular resonance, in which none of the particles remained inside the resonance for the whole length of the integration, caused some of the largest changes in proper  $e$  and  $\sin(i)$  observed when the particles switched from circulation to libration. The large number of weak secular resonances present in the region may, in principle, provide an additional mechanism of mobility in  $e$  and  $\sin(i)$  not considered in previous works and that may account for some of the differences between the dispersion in proper  $e$  and  $\sin(i)$  of observed and simulated families.

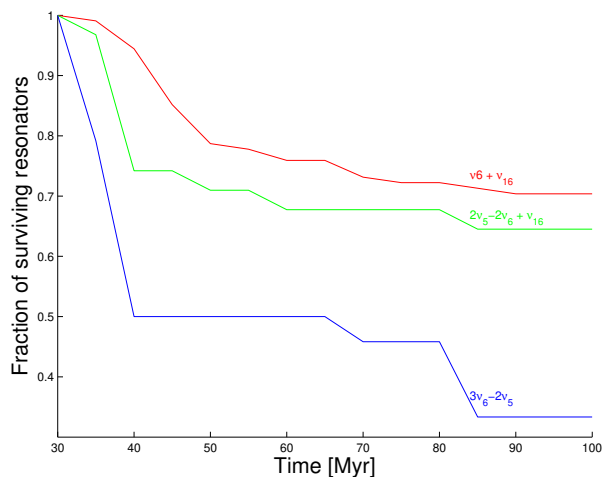
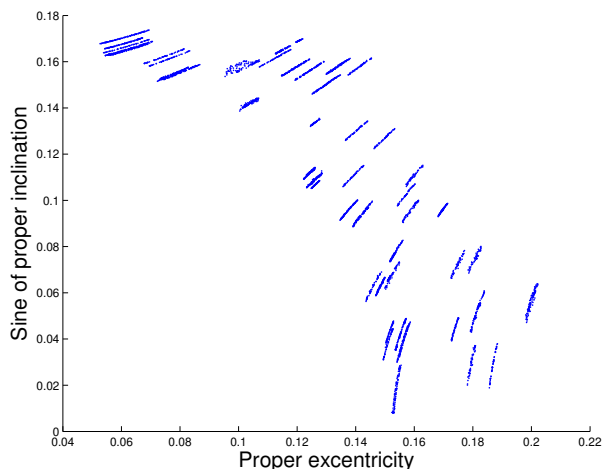
To better understand the long-term importance of evolution inside secular resonances we also performed longer simulations for the resonators inside the three secular resonances in the area with the largest population of librators: the  $3\nu_6 - 2\nu_5$ ,  $2\nu_5 - 2\nu_6 + \nu_{16}$ , and  $\nu_6 + \nu_{16}$  resonances. We computed the “sticking time”, defined as the time or permanence of particles inside each resonance, and the changes in proper  $e$  and  $\sin(i)$  associated with the passage through such commensurabilities. Fig 8 displays the fraction of surviving resonators as a function of sticking times for the three studied resonances: the longest times were observed for the  $\nu_6 + \nu_{16}$ , that also had the largest initial population of resonators (108, with respect to the 31 and 24 of the  $2\nu_5 - 2\nu_6 + \nu_{16}$  and  $3\nu_6 - 2\nu_5$  resonances, respectively). Other studied resonances had lower numbers of resonators and shorter sticking times.

Vokrouhlický *et al.* (2006b) introduced the modified quantity  $K_2' = \sqrt{1 - e^2}(2 - \cos i)$  that is conserved when the sole resonant gravitational perturbations are taken into account, and that was shown to be also preserved under the influence of the Yarkovsky effect for timescales of hundreds of Myr. Similar conserved quantities can be introduced for

<sup>3</sup> It should also be pointed out that many particles in resonances such as the  $3\nu_6 - 2\nu_5$  and the  $2\nu_5 - 2\nu_6 + \nu_{16}$  oscillate around more than one point of equilibrium, around  $0^\circ$  and  $180^\circ$ .

**Table 3.** Number of librators, mean and maximal value of time of permanence in resonance, change in proper  $e$  and  $\sin(i)$ , for the studied resonances

Resonance argument	Number of librators	mean $\Delta T$ [Myr]	max $\Delta T$ [Myr]	mean $\Delta e$	max $\Delta e$	mean $\Delta \sin(i)$	max $\Delta \sin(i)$
$3\nu_6 - 2\nu_5$	45	21.4	30	0.030	0.050	0.0041	0.0160
$2\nu_5 - 2\nu_6 + \nu_{16}$	96	22.6	30	0.008	0.070	0.0055	0.0900
$\nu_6 + \nu_{16}$	159	22.9	30	0.024	0.170	0.0105	0.0520
$\nu_5 + 2\nu_{16}$	15	13.8	30	0.024	0.080	0.0050	0.0013
$\nu_6 + 2\nu_{16}$	4	4.75	10	0.055	0.110	0.0002	0.0005
$2\nu_6 - \nu_5 + \nu_{16}$	29	16.17	30	0.007	0.035	0.0047	0.0400
$2\nu_6 - \nu_5 + \nu_{17}$	12	10.2	30	0.005	0.010	0.0004	0.0010

**Figure 8.** The fraction of surviving resonators inside the  $\nu_6 + \nu_{16}$  (red line),  $2\nu_5 - 2\nu_6 + \nu_{16}$  (green line), and  $3\nu_6 - 2\nu_5$  (blue line) secular resonances as a function of time.**Figure 9.** A proper ( $e, \sin(i)$ ) projection of the temporal evolution of particles that remained inside the  $z_1$  secular resonance for the whole length of the integration (100 Myr).

other secular resonances as well. Fig. 9 displays an ( $e, \sin(i)$ ) projection of the 56 time values of  $e$  and  $\sin(i)$  for the 76 particles that remained inside the  $z_1 = \nu_6 + \nu_{16}$  secular resonance for the whole length of the integration. It can be noticed that all particles followed lines of constant  $K_2'$  and oscillated between the maximum and minimum values of  $e$  and  $\sin(i)$  allowed by the conservation of  $K_2'$ , as it was also observed for analogous simulations of resonant particles in the region of the Padua family by Carruba (2009a).

The scenario is different for particles that escaped the  $z_1$  secular resonance. Fig. 10 displays the time evolution of proper eccentricity, sine of inclination, and an ( $e, \sin(i)$ ) projection of a particle that remained inside the  $z_1$  resonance for the whole length of the integration (panel A) and another one that escaped after 55 Myr (panel B). While the first particle displayed the characteristics anti-aligned oscillations in proper  $e$  and  $\sin(i)$ , the particle that escaped the secular resonance experienced a change in proper  $e$  and  $\sin(i)$  at the time of the separatrix crossing of 0.02 and 0.015, respectively. This abrupt and chaotic change caused by the crossing of this and several other secular resonances in the region is what may be causing part of the asteroid orbital drifting in proper  $e$  and  $\sin(i)$ .

## 5 CRONOLOGY

Having finished our preliminary investigation on mechanisms of dynamical mobility in the area of the Hygiea family, whose identification was discussed in Sect. 2, we are now ready to start addressing the issue of the family age. We will start by performing a preliminary analysis based on a simplified model of Yarkovsky drift (Vokrouhlický 1998, 1999).

### 5.1 Yarkovsky isolines

Vokrouhlický *et al.* (2006a,b,c) used the ( $a, H$ ) distribution of asteroid families to determine their ages. In particular, the authors introduced a parametric target function  $C$  defined as:

$$0.2H = \log_{10}(\Delta a/C), \quad (3)$$



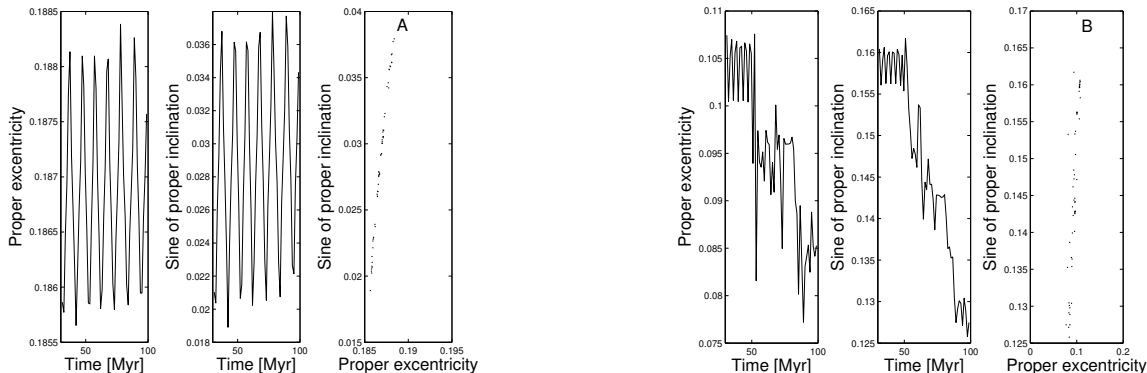


**Figure 10.** The time evolution of proper eccentricity, sine of inclination, and  $(e, \sin(i))$  of a particle that remained inside the  $z_1$  resonance for the whole length of the integration (panel A) and another one that escaped around 55 Myr (panel B).

where  $\Delta a = a - a_c$ , and  $a_c$  is the “central” value of semi-major axis of the family members. The authors used distributions of  $C$  values of observed asteroid families members for comparison, using  $\chi^2$  techniques, with results of Monte Carlo simulations of diffusion via Yarkovsky and Yarkovsky–O’Keefe–Radzievsky–Paddack (YORP) effects to obtain estimates of family age, and parameters associated with the strength of the initial ejection velocity field and YORP effect. In essence, the YORP effect forces the spin axes of asteroids to evolve towards the direction perpendicular to the orbital plane. In this configuration, the semi-major axis drift caused by the Yarkovsky effect is maximized. Asteroids either drift towards smaller  $a$  (if their rotation is retrograde) or larger  $a$  (if their rotation is prograde). This depletes the center of the family in the semi-major axis distribution.

The choice of using the absolute magnitude  $H$  was justified by the limited data then available on asteroids diameters and geometric albedo values. For instance, in Vokrouhlický et al. (2006a) the authors investigated four young families: Erigone, Massalia, Merxia, and Astrid. Only six albedo values were available for the Erigone family, and only two for the Merxia group, including an interloper. New results from the (Wright et al. 2010), and the NEOWISE (Mainzer et al. 2011) enhancement to the WISE mission allowed to obtain diameters and geometric albedo values for more than 100,000 Main Belt asteroids (Masiero et al. 2011). For the case of the Hygiea family, out of the 376 members of the halo, 280 have WISE values of diameters and geometric albedo  $p_V$ . Adopting the value of  $p_V$  of (10) Hygiea itself from the WISE mission (that is actually extremely close to the mean value of geometric albedo of the family, see Sect. 2), Eq. 2 can be used to estimate the diameters of the remaining 96 objects. Since Pravec et al. (2012) have also presented evidence of possible biases in the various catalogs of asteroid absolute magnitudes, in this work we choose to modify Eq. 3 by computing new “WISE revised” values of absolute magnitudes  $H_{rev}$  with the formula:

$$H_{rev} = 15.617 - 5 \cdot \log_{10}(2R) - 2.5 \cdot \log_{10}(p_V), \quad (4)$$

where  $R$  is the value of the asteroid radius from the WISE mission. For asteroids without WISE data on  $R$  and  $p_V$ , we kept the AstDys published value of  $H$ .

A problem in obtaining reliable  $C$  values resides in the determination of the family “center”. The most appropriate definition of family center relates to the concept of barycen-

**Table 4.** Location in proper elements  $(a, e, \sin(i))$  domain of the barycenter of (10) Hygiea, the Hygiea family core and halo

Group	$a_{barycenter}$	$e_{barycenter}$	$\sin(i)_{barycenter}$
(10) Hygiea	3.1262	0.1493	0.0895
Hygiea family core	3.1390	0.1346	0.9144
Hygiea family halo	3.1423	0.1224	0.0953

ter (Carruba 2010a,b). Simulations of asteroid dynamical groups in the orbital region of the Phocaea family showed that, while the orbital position of individual asteroids can be modified with time by several mechanisms of orbital mobility, the position of the family barycenter tends to remain relatively stable, and changes less than the position of the family center. To compute the barycenter in proper  $a$  we took

$$a_c = \sum_{i=1}^{n_{ast}} \frac{a \cdot M_i}{M_{tot}}, \quad (5)$$

where  $n_{ast}$  is the number of family members, and  $M_i$  is the mass of each asteroid, estimated assuming that all asteroids can be approximated as spheres, using the density of  $2080 \text{ kg/m}^3$  reported by Baer et al. (2011) for (10) Hygiea, and the diameters from the WISE and NEOWISE missions, when available (we used the results from Eq. 2 with the geometric albedo value of (10) Hygiea for the other 96 cases). Eqs. similar to Eq. 5 hold for proper  $e$  and  $i$ .

We computed the location of the barycenter of the family core and halo, with and without (10) Hygiea, which holds more than 95% of the mass of the family. Expectedly, if we include (10) Hygiea, the position of the family barycenter differs little from that of (10) Hygiea itself. Nevertheless, if we exclude this asteroid and other objects unlikely to be members for dynamical reasons that will be explained later on in this section, there is a discrepancy in the position of the barycenter of  $0.016 \text{ AU}$  with respect to the current loca-

tion of (10) Hygiea. Since the family shows an asymmetry, with more objects at larger  $a$  than at lower  $a$ , if we put the center of the family at the current orbital location of (10) Hygiea, we believe that a possible reason for this discrepancy could be that the current position of (10) Hygiea is not the one that this asteroid occupied when the family formed. While the Yarkovsky drift for a body this size ( $D = 453.2 \text{ km}$ , Masiero et al. 2011) is practically infinitesimal even on timescales of the order of the age of the Solar System, in paper II it was observed that (10) Hygiea experienced close encounters with (1) Ceres, (2) Pallas, (4) Vesta and other massive asteroids that could account for a displacement in proper  $a$  of this asteroid of the observed amount. The discrepancy between the current position of the barycenter of the family (without (10) Hygiea) and the current position of (10) Hygiea itself could be a “fossil” proof of past dynamical mobility of the orbit of this asteroid caused by close encounters with massive asteroids<sup>4</sup>. Table 4 summarizes the results of our analysis, with values of the barycenter location in proper  $a$ ,  $e$  and  $\sin(i)$  for (10) Hygiea and other dynamical interlopers) core and halo, as obtained in Sect. 2. Almost all the mass of the family is concentrated in (10) Hygiea, with only 0.57% of the total mass in halo members, and 0.34% in core members.

We then turned our attention to the Yarkovsky isolines method to obtain asteroid age estimates and the  $C$ -parameter distribution. Fig. 11, panel A, displays a proper  $a$  versus radius  $R$  projection of members of the Hygiea family halo (results are similar in terms of age determination for Hygiea family core members and won’t be shown for simplicity; also, with a radius of  $226.6 \text{ km}$  (10) Hygiea itself is out of the range of this picture). The red and blue curves show isolines of maximum displacement in  $a$  caused by the Yarkovsky effect, computed using the Vokrouhlický (1998, 1999) model of the diurnal version of the Yarkovsky effect, for spherical bodies and in the linear approximation for the heat conduction in a spherical, solid, and rotating body illuminated by solar radiation, for a fictitious family originally centered in the family barycenter after 3.0 Byr (red line) and 4.4 Byr (blue line). We used the following parameters to describe the Yarkovsky force: a value of thermal conductivity  $K = 0.001 \text{ W/m/K}$ , a specific heat capacity of  $C_p = 680 \text{ J/kg/K}$ , a density of  $2080 \text{ kg/m}^3$ , a surface density of  $1500 \text{ kg/m}^3$ , a bond albedo of 0.11, the geometric albedo from the WISE mission when available (otherwise we used the value of geometric albedo of (10) Hygiea), and the diameters of halo and core members previously computed. We eliminated all C-, B-, and X-type asteroids whose distance from the family barycenter was larger than the maximum Yarkovsky drift over 4.5 Byr plus  $0.02 \text{ AU}$ , the maximum displacement caused by close encounters with (10) Hygiea observed in paper II. Asteroids (52) Europa, (106)

<sup>4</sup> Other possible explanation of this asymmetry include an oblique collision between the impactor and the parent body of the Hygiea family, or the possible existence of multiple Hygiea families, caused by successive collisions. In this work we prefer to investigate what, in our opinion, is the simpler scenario, that involves a non atypical ejection velocity field, a single Hygiea family, and a limited amount of dynamical mobility for (10) Hygiea itself.

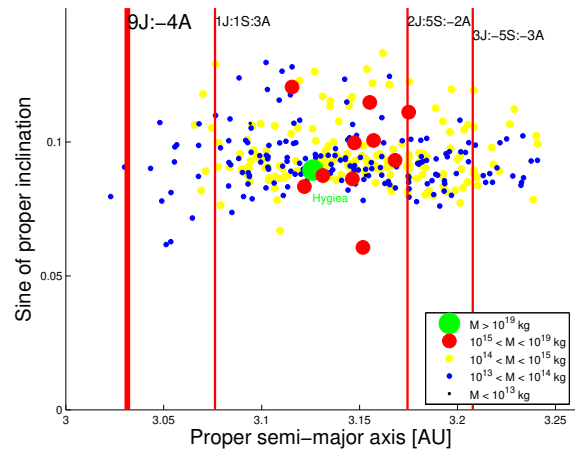


**Figure 12.** An  $(a, \sin(i))$  projection of the Hygiea halo members. The sizes of the dots are proportional to the asteroid mass.

Dione, (159) Aemilia, (211) Isolda, (538) Friederike, (867) Kovacia, (1107) Lictoria, (1599) Giomus, (2436) Hatshepsut, (6644) Jugaku, (9544) Scottbirney, (16093) (1999 TQ180), and (16450) Messerschmidt were considered dynamical interlopers, and their mass was not considered in the computation of the mass of the family and of the family barycenter. After this analysis, we were left with a sample of 267 and 363 possible Hygiea family members in the core and in the halo, respectively. Fig 12 displays an  $(a, \sin(i))$  projection of the halo members, with the sizes of the dots displayed according to the asteroid mass. As previously discussed, more than 99% of the family mass is owned by (10) Hygiea itself.

Yarkovsky isolines will not give a very reliable estimate of the age of the family, since they do not account for the original dispersion at break-up moment (all asteroids are assumed to be originally at the barycenter of the family) and do not consider the effect of reorientations and YORP cycles (Vokrouhlický and Čapek 2002, Čapek and Vokrouhlický 2004), but they will give a preliminary value that can later on be refined by more advanced method, as the ones discussed in the next sections. The Hygiea family seems to be a relatively old group, with an age at least larger than 3.0 Byr. Since modeling of YORP cycle and effect of reorientations are not reliable for ages larger than  $\simeq 1.0 \text{ Byr}$  (Vokrouhlický et al. 2006a,b), a very accurate determination of the family age seems to be not likely to occur. Nevertheless, we will try in the next sub-section to further refine this initial order of magnitude estimation.

Fig. 11, panel B shows a histogram of the values of the  $C$  target function for the Hygiea family halo members computed with Eqs. 3 and 4, after our process of elimination of taxonomical and dynamical interlopers. We used 38 intervals starting at  $C_{min} = -1.5 \cdot 10^{-4}$  with a step of  $8.0 \cdot 10^{-6} \text{ AU}$ . We computed an average  $C$  distribution for the halo family obtained as a mean of the computed values for  $a_c$  in the interval  $[3.140, 3.144] \text{ AU}$  around the family barycenter (computed without (10) Hygiea and dynamical interlopers). This was done to avoid random fluctuations in the  $N(C)$  distribution that would affect the quality of the fit. The Hygiea family seems to show a not very pronounced bimodal distribution of  $C$  values, typical of Yarkovsky/YORP evolved asteroid families. Synthetic distributions of the  $C$  function

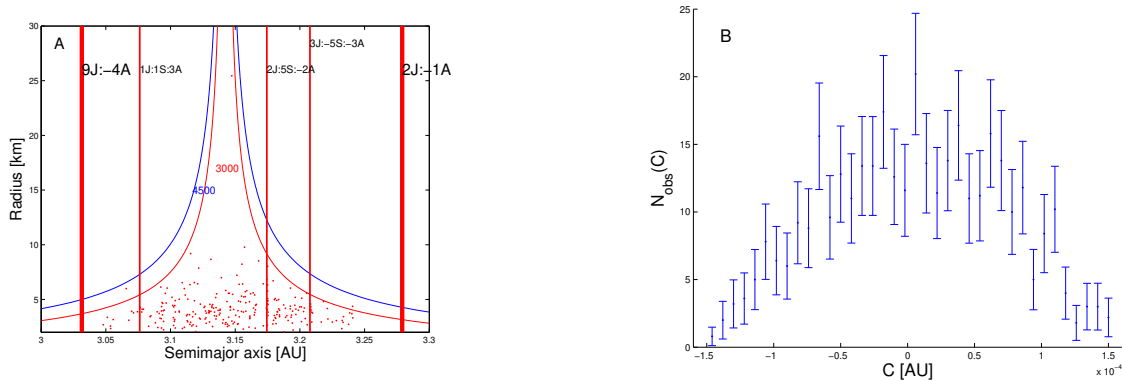


**Figure 11.** Panel A: a proper  $a$  versus radius projection of members of the Hygiea family halo. The red and yellow curves show isolines of maximum displacement in  $a$  caused by Yarkovsky effect for a fictitious family originally centered in the family barycenter after 3.0 Byr (red line) and 4.5 Byr (blue line). Panel B: values of the  $C$ -target function for the same objects. The error bars are given as  $\sqrt{N_{obs}(C)}$  for each interval  $(C, C + \Delta C)$ , with  $\Delta C = 8.0 \cdot 10^{-6}$  AU.

will be obtained using Monte Carlo simulations of Yarkovsky and YORP dynamical mobility of fictitious family members in the next sub-section.

## 5.2 Monte Carlo simulations

In this section we will analyze the semi-major axis evolution of the Hygiea halo family members. The methods used here follow the work of Vokrouhlický *et al.* (2006a, b), that showed that the skewed  $a$ -distribution of asteroid family members may be explained as a consequence of the Yarkovsky -O’Keefe -Radzievsky -Paddack (YORP) effect. Asteroids have their spin axes evolved to alignments perpendicular to the orbital plane, which accelerates the migration of asteroids and depletes the family center. Modeling the evolution of asteroid members as a function of the parameters that characterize the Yarkovsky and YORP evolution of the asteroids (age of the family, YORP strength ( $C_{YORP}$ ), the characteristic ejection velocity  $V_{EJ}$  given by

$$V_{SD} = V_{EJ} \cdot (5km/D), \quad (6)$$

where  $V_{EJ}$  is a free parameter characterizing the size of the family in velocity space and  $D$  is the asteroid diameter, may produce a distribution of semimajor axis values, that can then be transformed into a  $C$ -distribution using Eq. 3. Using the values of Yarkovsky parameters discussed in the previous subsections, the simulated  $C$ -distributions can then be compared to the observed one, and minimizing the  $\chi^2$ -like function:

$$\psi_{\Delta C} = \sum_{\Delta C} \frac{[N(C) - N_{obs}(C)]^2}{N_{obs}(C)}, \quad (7)$$

the best-fit values of the Yarkovsky and YORP model can be obtained. Since the predicted age of the Hygiea family is higher than 1.0 *Byr*, a value for which the current understanding of the YORP cycle is not very accurate, and since past experiences with this method showed us that is not very dependent on the value of the  $C_{YORP}$  parameter, provided is not zero (Carruba 2009a, Masiero *et al.* 2012), we will assume a value of  $C_{YORP} = 1.0$ , and will limit our analysis to a two-dimensional parameter space defined by the age of the family and its characteristic ejection velocity

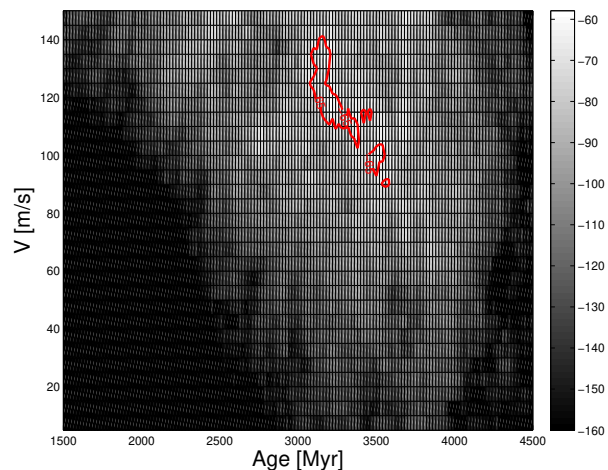


**Figure 13.** Values of the target function  $\psi_{\Delta C}$  in the  $(Age, C_{YORP})$  plane for member of the Hygiea family halo.

$V_{EJ}$ . Admissible solutions are characterized by  $\psi_{\Delta C}$  of the order of the number of used bins in  $C$  (38, in our case), while solutions giving much larger  $\psi_{\Delta C}$  are incompatible with the observed family. To quantify the goodness of the fit, we used the incomplete gamma function  $\Gamma(N_{int}, \psi_{\Delta C})$  (Press *et al.* 2001), where  $N_{int} = 38$  is the number of intervals used for the values of the  $C$  target function and  $\psi_{\Delta C}$  was computed with Eq. 7. We used a value of  $\psi_{\Delta C}$  of 65 as a limit for an acceptable fit (red line in Fig. 13, as this would correspond to a probability of 99.67% that the simulated distribution differs from the observed (Press *et al.* 2001).

Fig. 13 shows the values of the target function  $\psi_{\Delta C}$  in the  $(Age, V)$  plane<sup>5</sup>. The predicted age and the characteristic ejection velocity field  $V_{EJ}$  of members of the Hygiea family halo are in the range  $T = 3200^{+380}_{-120}$  My and  $V_{EJ} = 115 \pm 26$  m/s, and results are similar for the Hygiea family core. Estimates of the Hygiea family age obtained with Monte Carlo simulation are in good agreement with

<sup>5</sup> To associate lower levels of  $\psi_{\Delta C}$  with whither tones we plotted color plots of  $-\psi_{\Delta C}$ .

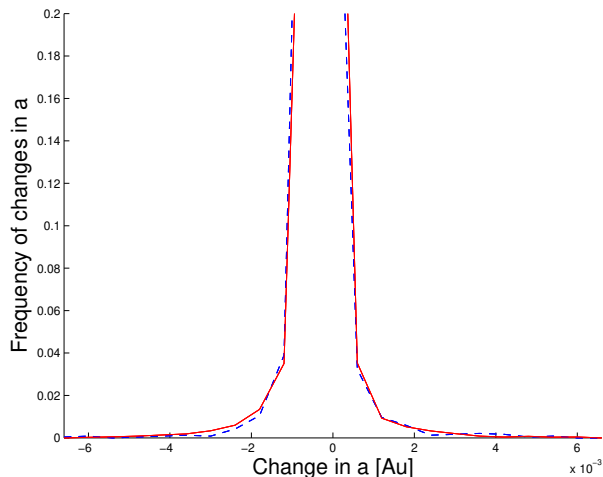


**Figure 14.** A histogram of the *pdf* curve obtained in Sect. 3 (red curve) and of of the new probability distribution function obtained with the rejection method (blue dotted line).

results obtained with the simpler approach described in 5.1, and with those reported by Nesvorný et al. (2005). The relatively high value of the ejection velocity parameter, unusual for families associated with the break-up of the parent body, is however typical of families created by cratering events, such as the Vesta and the Hygiea groups.

### 5.3 Effects of close encounters on Hygiea family chronology

As a next step in our analysis of the dynamical evolution of the Hygiea family, we investigated the effects that close encounters with (10) Hygiea may have on the estimate of the family age. For this purpose we first best-fitted polynomials of order eight to the *pdf* distribution of changes in proper  $a$  (as obtained in Sect. 3) between the values  $0.0006 < |\Delta a| < 0.006$  AU, and a gaussian with the measured values of standard deviation in proper  $a$  of  $8.9 \cdot 10^{-4}$  AU for the central values. We then replicated the observed distribution using the rejection method (Press et al. 2001), with appropriate Lorentzian distributions as comparison probabilities distribution functions.

Fig. 14 displays a histogram of the *pdf* curve obtained in Sect. 3 (red curve) and of of the new probability distribution function obtained with the rejection method (blue dotted line), computed over 23 equally spaced intervals between  $\pm 0.0066$  AU. Percentual differences between values of the two distributions are less than 1%. We then performed new Monte Carlo simulations of the dynamical evolution of synthetic Hygiea family members, that include this time the effect of close encounters with (10) Hygiea. We computed changes in semi-major axis caused by the computed *pdf* after each 120.2 Myr, time sufficient for having a  $2\sigma$ -compatible *fdf* and a population of close encounters equal to seven times the number of Hygiea halo members, by applying seven times the computed *pdf*, and obtaining a resulting cumulative change in proper  $a$  for each of the 363 members of the Hygiea halo.

Fig. 15 shows the values of the target function  $\psi_{\Delta C}$  in the  $(Age, V)$  plane for this new set of simulations. We used

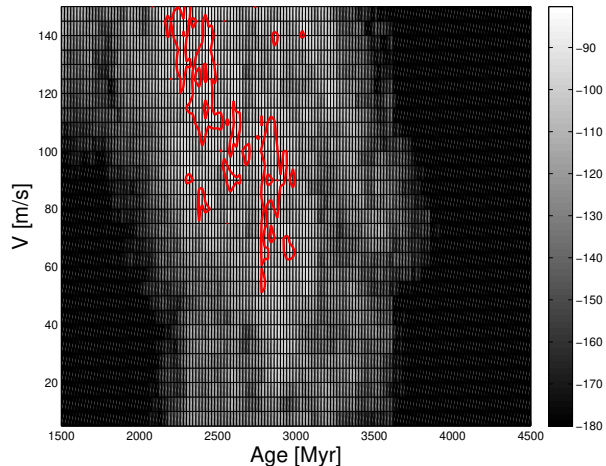


**Figure 15.** Values of the target function  $\psi_{\Delta C}$  in the  $(Age, C_{YORP})$  plane for member of the Hygiea family halo, evolved under the influence or Yarkovsky and YORP effects, and close encounters with (10) Hygiea.

a value of  $\psi_{\Delta C}$  of 93 as a limit for an acceptable fit (red line in Fig. 15). The predicted age and the characteristic ejection velocity field  $V_{EJ}$  of members of the Hygiea family halo are now in the range  $T = 2420^{+580}_{-270}$  Myr and  $V_{EJ} = 135^{+15}_{-85}$  m/s, and results are similar for the Hygiea family core. Surprisingly, we found that, with respect to the simulations without close encounters with (10) Hygiea, the estimated age of the family is 780 Myr younger, which corresponds to a change of 24.4%. This new result poses new interesting questions on the importance of close encounters for the dynamical evolution of asteroid families around massive bodies, such as the Hygiea, Vesta, Gefion, and, possibly, the Pallas family.

## 6 CONCLUSIONS

In this work we:

- Performed a taxonomical analysis of members of the Hygiea family (core and halo) as obtained in Carruba (2013), with the DeMeo and Carry (2013) approach. We identified 276 and 376 members of the Hygiea family core and halo, respectively, whose taxonomy is compatible with membership in this family (types C-, X-, and B-), and have  $H < 13.5$ . Except for B-type objects, that may possibly be associated with the Hygiea and Themis family, C- and X-types bodies in the Hygiea halo cannot univocally be associated with the break-up of the Hygiea parent body, but can possibly also be originating from the Veritas or Themis families.

- Studied the long-term effect of close encounters with (10) Hygiea on the dynamical evolution of members of its halo. We confirmed the prediction of Carruba et al. (2013) that the frequency distribution function (*fdf*) of changes in  $a$  converges to the probability distribution function (*pdf*) for number of encounters of about 6000 (5455). The populations of Hygiea family halo and core identified with the DeMeo and Carry (2013) approach are expected to experience a number of encounters sufficient to obtain a  $2\sigma$  level (or 95.4%) approximation of the *pdf* in 113.1 and 162.3 Myr, respectively.

- Studied the effect of secular dynamics in the region of the Hygiea asteroid family. The secular resonances that cross the dynamical family, such as the  $\nu_5 + 2\nu_{16}$ ,  $\nu_6 + 2\nu_{16}$ ,  $2\nu_6 - \nu_5 + \nu_{16}$ , and  $2\nu_6 - \nu_5 + \nu_{17}$  resonances, have a limited current population of resonators and relatively short sticking times. Furthermore, they influence the orbital evolution of Hygiea family members mostly by the occasional relatively large change in proper elements caused by the crossing of the resonance separatrix. Of the three most populated secular resonances studied in Carruba 2013, the  $3\nu_6 - 2\nu_5$ ,  $2\nu_5 - 2\nu_6 + \nu_{16}$ , and  $\nu_6 + \nu_{16}$  resonances, the  $z_1 = \nu_6 + \nu_{16}$  resonance has the largest current population of resonators and the longest sticking times.

- Obtained a preliminary estimate of the age of the Hygiea family based on the method of Yarkovsky isolines of at least 3.0 Byr. We found that (10) Hygiea itself is not located at the current position of the barycenter of the family, but it is displaced by 0.016 AU. This may indicate that it experienced dynamical mobility since the formation of the family, possibly caused by close encounters with some other massive asteroids since Yarkovsky mobility is negligible for a body of its size.

- We performed Monte Carlo simulations of the dynamical mobility caused by the Yarkovsky and YORP effects of synthetic Hygiea family members following the approach of Vokrouhlický *et al.* (2006a, b). The predicted age and the characteristic ejection velocity field  $V_{EJ}$  of members of the Hygiea family halo are in the range  $T = 3200^{+380}_{-120}$  Myr and  $V_{EJ} = 115 \pm 26$  m/s, and results are similar for the Hygiea family core, and in agreement with previous estimates (Nesvorný *et al.* 2005).

- We modeled the long-term effect of close encounters on the dynamical evolution in semi-major axis of members of the Hygiea family halo. Surprisingly, we found that including close encounters as a mechanism of dynamical mobility could reduce the estimated age of the Hygiea asteroid family by  $\simeq 25\%$ . This poses new interesting questions on the importance of close encounters on the dynamical evolution of asteroid families around massive bodies, such as the Hygiea, Vesta, Gefion, and, possibly, the Pallas family.

As a by-product of our taxonomical analysis of the Hygiea family halo, we identified, very surprisingly, one possible V-type candidate: the asteroid (177904) (2005 SV5). If confirmed, this could be the fourth V-type object ever to be identified in the outer main belt.

While in this work we obtained the first estimate of the Hygiea family age that we are aware of, we would like to emphasize that this estimate is affected by several uncertainties: Masiero *et al.* (2012) showed that changes in the values of thermal conductivities and mean densities of family members can change the estimated value of the family age by up to 40%. Other effects such the progressive change in surface properties caused by space weathering, the change in solar luminosity in the past (Bahcall *et al.* 2001), and, possibly, low energy collisions (Dell’Oro and Cellino 2007) all may play a role in affecting the estimated age of the family. While we do not yet have a good understanding of how to model the space weathering effect on C-, B-, and X-type asteroids, the effect of changes in solar luminosity affects the estimated age of the family by at most 4% (Vokrouhlický *et al.* 2006b), and the effect of low-energy collisions seems to

be a minor one (Carruba 2009a), of most importance however, are the current limitations on our understanding of the YORP effect. Cotto-Figueroa *et al.* (2013) have shown that the YORP effect has an extreme sensitivity to the topography of asteroids. If the spin-driven reconfiguration leads to a shape of the aggregate that is nearly symmetric, the YORP torques could become negligibly small or even vanish. This would imply a self-limitation in the evolution of the spin state and the objects would not follow the classical YORP cycle. Since our understanding of YORP cycles may be not adequate for modeling the evolution of family members on very long time scales, we preferred not to conduct extensive simulations with symplectic integrators in order to better refine the age estimate of the Hygiea family.

Whatever the best way to account for all the limitations on our modeling of the long-term effects of Yarkovsky and YORP effect could be, here for the first time we showed the importance that close encounters with massive asteroids may also have for the dynamical evolution of the Hygiea family, and how they could reduce the estimated age of this family by  $\simeq 25\%$ . This opens new and interesting perspectives for investigating the ageing process of asteroid families, that could be best investigated by studying younger families with relatively massive parent bodies, such as, possibly, the Massalia family (Vokrouhlický *et al.* 2006a).

## ACKNOWLEDGMENTS

We thank the reviewer of this paper, Ricardo Gil-Hutton, for comments and suggestions that significantly increased the quality of this work. We also would like to thank the São Paulo State Science Foundation (FAPESP) that supported this work via the grant 11/19863-3, and the Brazilian National Research Council (CNPq, grant 305453/2011-4). This publication makes use of data products from the Wide-field Infrared Survey Explorer, which is a joint project of the University of California, Los Angeles, and the Jet Propulsion Laboratory/California Institute of Technology, funded by the National Aeronautics and Space Administration. This publication also makes use of data products from NEOWISE, which is a project of the Jet Propulsion Laboratory/California Institute of Technology, funded by the Planetary Science Division of the National Aeronautics and Space Administration.

## REFERENCES

- Baer, J., Chesley, S. R., Matson, R. D. 2011, *AJ*, 141, 143.  
 Bahcall, J. N., Pinsonneault, M. H., & Basu, S., 2001, *ApJ*, 555, 990.  
 Brož, M., 1999, Thesis, Charles Univ., Prague, Czech Republic.  
 Čapek, D., & Vokrouhlický, D. 2004, *Icarus*, 172, 526.  
 Carruba V., Burns, J. A., Bottke, W., Nesvorný, D. 2003, *Icarus*, 162, 308.  
 Carruba, V., Michtchenko, T. A. 2007, *A&A*, 475, 1145.  
 Carruba V., 2009a, *MNRAS*, 395, 358.  
 Carruba V., 2010a, *MNRAS*, 403, 1834.  
 Carruba V., 2010b, *MNRAS*, 408, 580.

- Carruba, V., Huaman, M., Douwens, S., Domingos, R. C., 2012, *A&A*, 543, A105.
- Carruba V., Huaman, M. E., Domingos, R.C., Roig, F. 2013a, *A&A* 550, A85.
- Carruba V., 2013, *MNRAS*, 431, 3557.
- Carruba V., Domingos, R.C., Nesvorný, D., Roig, F., Huaman, M. E., Souami, D., 2013b, *MNRAS*, 433, 2075.
- Cotto-Figueroa, D., Statler, T. S., Richardson, D. C., Tanga, P. 2013, *DDA*, 102.02.
- Dell’Oro, A., Cellino A. 2007. *MNRAS*, 380, 399.
- DeMeo, F., Carry, B. 2013, *astro-ph*, arXiv:1307.2424.
- Duffard, R., *Earth Moon Planet.* 105, 221.
- Farinella, P., Vokrouhlický, D., Hartmann, W. K., 1998, *Icarus*, 132, 378.
- Greenberg, R. 1982. *AJ*, 87, 184.
- Holmberg, J., Flynn, C., Portinari, L., 2006, *MNRAS*, 367, 449.
- Knežević, Z., Milani, A., 2003, *A&A*, 403, 1165.
- Ivezić, Ž, and 34 co-authors, 2002, *AJ*, 122, 2749.
- Levison, H. F., Duncan, M. J., 1994, *Icarus*, 108, 18.
- Machuca, J. F., Carruba, V., 2011, *MNRAS*, 420, 1779.
- Mainzer, A. K., and 35 co-authors, 2011, *ApJ*, 731, 53.
- Masiero, J. R., and 17 co-authors, 2011, *ApJ*, 741, 68.
- Masiero, J. R., Mainzer, A. K., Grav, T., Bauer, J. M., and Jedicke, R., 2012, *AJ*, 759, 14.
- Mothé-Diniz, T., Roig, F. Carvano, J. M. 2005, *Icarus*, 174, 54.
- Neese, C., 2010, *Asteroid Taxonomy*, NASA Planetary Data System, eAR-A-5-DDR-TAXONOMY-V6.0.
- Nesvorný, D., Jedicke, R., Whiteley, R. J., Ivezić, Ž., 2005, *Icarus*, 173, 132.
- Pravec, P., Harris, A., W., Kušnirák, P., Galád, A., Hornoch, K., 2012, *Icarus*, 221, 365.
- Press, V.H., Teukolsky, S. A., Vetterlink, W. T., Flannery, B. P., 2001, *Numerical Recipes in Fortran 77*, Cambridge Univ. Press, Cambridge.
- Vokrouhlicky, D. 1998, *A&A*, 335, 1093.
- Vokrouhlický D. 1999, *A&A* 344,362.
- Vokrouhlický, D., & Čapek, D. 2002, *Icarus*, 159, 449.
- Vokrouhlický, D., Brož, M., Morbidelli, A., et al. 2006a, *Icarus*, 182, 92.
- Vokrouhlický D., Brož, M., Bottke, W. F., Nesvorný, D., Morbidelli, A. 2006b, *Icarus*, 182, 118.
- Vokrouhlický D., Brož, M., Bottke, W. F., Nesvorný, D., Morbidelli, A. 2006c, *Icarus*, 183, 349.
- Vokrouhlický D., Brož, M., Morbidelli, A., Bottke, W. F., Nesvorný, Lazzaro, D., Rivkin, A. S., 2006d, *Icarus*, 182, 92.
- Wright, E. L., and 38 co-authors, 2010, *AJ*, 140, 1868.

This paper has been typeset from a  $\text{\TeX}$ / $\text{\LaTeX}$  file prepared by the author.

